



Feasibility of a novel technique using 3-dimensional modeling and augmented reality for access during percutaneous nephrolithotomy in two different ex-vivo models

Murat Akand^{1,7} · Levent Civcik² · Ahmet Buyukaslan³ · Emre Altintas¹ · Erdinc Kocer⁴ · Mustafa Koplay⁵ · Tibet Erdogru⁶

Received: 17 September 2018 / Accepted: 19 November 2018 / Published online: 24 November 2018
© Springer Nature B.V. 2018

Abstract

Purpose We describe a novel technique that uses mathematical calculation software, 3-dimensional (3D) modeling and augmented reality (AR) technology for access during percutaneous nephrolithotomy (PCNL) and report our first preliminary results in two different ex-vivo models.

Methods Novel software was created in order to calculate access point and angle by using pre-operative computed tomography (CT) obtained in 50 patients. Two scans, 27 s and 10 min after injection of contrast agent, were taken in prone PCNL position. By using DICOM objects, mathematical and software functions were developed to measure distance of stone from reference electrodes. Vectoral 3D modeling was performed to calculate the access point, direction angle and access angle. With specific programs and AR, 3D modeling was placed virtually onto real object, and the calculated access point and an access needle according to the calculated direction angle and access angle were displayed virtually on the object on the screen of tablet.

Results The system was tested on two different models—a stone placed in a gel cushion, and a stone inserted in a bovine kidney that was placed in a chicken—for twice, and correct access point and angle were achieved at every time. Accuracy of insertion of needle was checked by feeling crepitation on stone surface and observing tip of needle touching stone in a control CT scan.

Conclusions This novel device, which uses software-based mathematical calculation, 3D modeling and AR, seems to ensure a correct access point and angle for PCNL. Further research is required to test its accuracy and safety in humans.

Keywords Percutaneous nephrolithotomy · Access · 3-Dimensional · Augmented reality · Software · Modeling

Murat Akand and Levent Civcik contributed equally to this work, and therefore are the first co-authors of the article.

✉ Murat Akand
drmuratakand@yahoo.com

¹ School of Medicine, Department of Urology, Selcuk University, Konya, Turkey

² Higher School of Vocational and Technical Sciences, Department of Computer Technologies, Selcuk University, Konya, Turkey

³ Konya Teknokent, AE Kod Teknolojisi, Konya, Turkey

Introduction

Percutaneous nephrolithotomy (PCNL) is considered to be the first line of treatment not only for stones bigger than 2 cm, but also stones resistant to or not appropriate for shock wave lithotripsy [1]. The basis of PCNL depends

⁴ Technical Education Faculty, Department of Electronic and Computer Education, Selcuk University, Konya, Turkey

⁵ School of Medicine, Department of Radiology, Selcuk University, Konya, Turkey

⁶ UroKlinik -Center of Excellence in Urology, Istanbul, Turkey

⁷ Selçuk Üniversitesi, Alaeddin Keykubat Kampüsü, Tıp Fakültesi Hastanesi, E-Blok, Kat:1, Üroloji Polikliniği, Selçuklu, 42075 Konya, Turkey

on removal of a stone causing obstruction by developing a nephrostomy tract during an operation in 1941 by Rupel and Brown [2]. Although Goodwin et al. reported in 1955 that drainage with a percutaneous nephrostomy could be used in the management of obstruction and infection, it has taken 20 years to use a percutaneous tract specifically for a successful endoscopic removal of a stone [3, 4]. Since the first series of PCNL was reported by Wickham in 1981, PCNL has become more commonly used world wide due to the evolvement in its technique and instrumentation, and its advantages such as short hospitalization time, low morbidity rates, high success rates and low costs [5, 6]. Although PCNL has a higher morbidity when compared to shock wave lithotripsy and ureterorenoscopy, its efficacy has not been yet beaten by the other minimally invasive modalities.

Establishing a good access is the first and probably the most important step of this procedure, which is challenging and has the steepest learning curve. Creating an appropriate access into the collecting system is crucial for successful removal of stone(s) with no or minimal complications, and requires a thorough understanding of the perirenal and renal anatomy. Puncture of the targeted calyx can be guided by fluoroscopy, ultrasound, or a combination of both with their own advantages and disadvantages, and no consensus exists which modality is superior to the other one [7]. Several technical modifications and navigation concepts have been proposed to ease this step, such as robotic assistance [8, 9], laser positioning device [10], virtual projection of ultrasound images onto fluoroscopic images [11], computer-assisted gantry system [12], stereotactic needle guidance system [13], mechanical apparatus assisting needle placement [14], electromagnetic tracking systems [15, 16], laser-guided puncture with the Uro Dyna-CT [17], iPad-assisted access [18], and pre-operative 3-dimensional (3D) model construction [19]. However, thus far, none of these ideas have been widely accepted in clinical routine, mainly because of poor cost-effectiveness, complex technique, or need for additional sophisticated equipment.

Herein, we describe a novel technique that uses 3D modeling and augmented reality (AR) technology to establish an access during PCNL, and report our first preliminary results in two different ex-vivo models.

Materials and methods

The study was performed in accordance with the ethical standards laid down in the 1964 Declaration of Helsinki and its later amendments. The protocol was approved by the Ethics Committee of Selcuk University (approval number: 2013/7, approval date: 13.03.2013).

In order to calculate the access point and angle, novel special software has been created by our team (A.B., L.C.,

E.K.). Use of real patient data was planned to perform the calculations and mathematical modeling; therefore, a pre-operative computed tomography (CT) was obtained in 50 patients who were planned to undergo PCNL for kidney stone(s) after receiving their written informed consent.

The CT was taken in prone position where two gel cushions were positioned under the chest of the patient as in PCNL. Two scans, 27 s and 10 min after the injection of the contrast agent, were taken with dual-source dual-energy 256-channeled CT device (Somatom Definition Flash®, Siemens, Germany), where four pointer electrodes were placed on the lumbar region of the patient.

By using the DICOM objects generated from the CT scans, mathematical and software functions (“PCNL Calculation program”) were developed to measure the distance of the stone from the reference electrode. First, the distances on the images in DICOM format were measured in a 1:1 ratio, in which a “pixel to millimeter” conversion was required. This conversion for standard 300 dots per inch (dpi) was done with the following formula:

$$mm = \frac{pixels \times 25.4}{dpi}$$

The calculation of the access angle, access point and direction angle can be summarized in two main subparts (i–iv and v–ix) as follow (Fig. 1a–c):

- i. Point A represents the location of the stone (the point where the needle is wanted to touch the stone or inside of the collecting system = touching point), point B is the projection point of the stone on the surface of the model, point C is the reference electrode chosen randomly among the pointer electrodes, and point D represents the projection point of the reference electrode on the same vertical axis with B (in other words, the point used for calculation where B is projected to be on the same horizontal axis with C).
- ii. The distance between C and D (k) is calculated by multiplying the difference between DICOM number of the reference electrode and DICOM number of the projection of the reference electrode with CT slice interval (DICOM files interval) (s).

Calculated length—1:

$$k = (\#DICOM_C - \#DICOM_D) \times s$$

- iii. The distance between D and B (l) can be measured with the “LINES” command of the DICOMVCL application.

Measured length—1:

$$l = LINES(D - B)$$

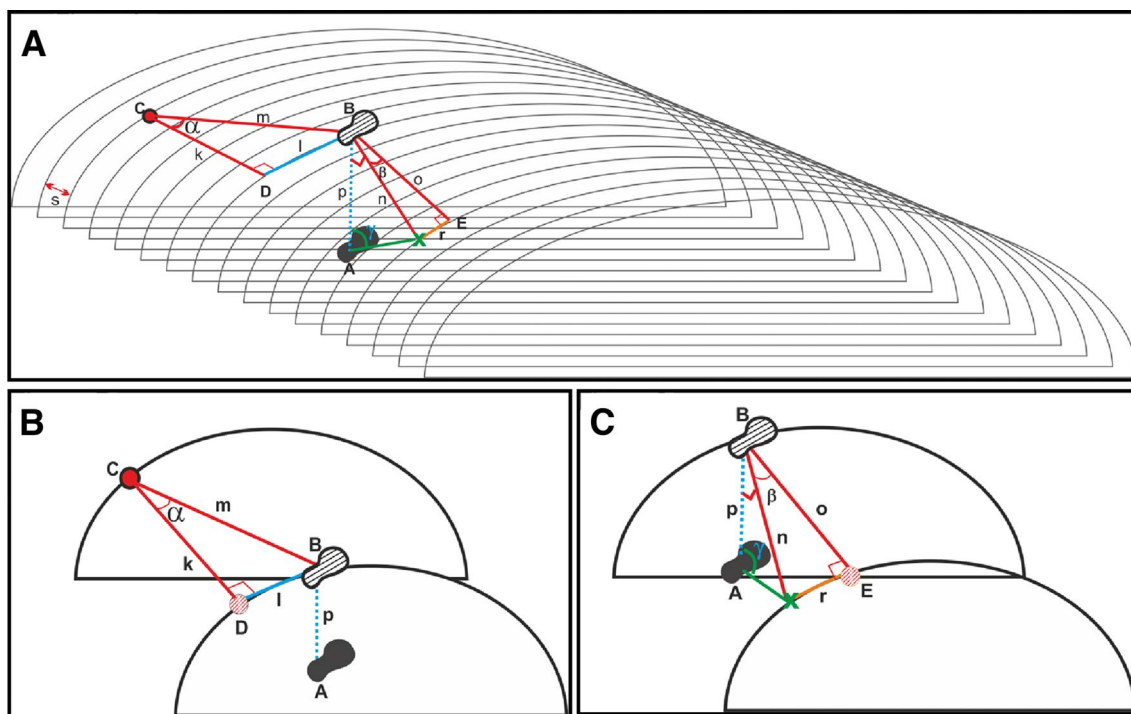


Fig. 1 Schematic explanation of the calculation of the distances and the access point, direction angle and access angle. **a** General view. **b** The calculation steps of i–iv. **c** The calculation steps of v–ix. *Point A*: stone (touching point). *Point B*: projection point of stone. *Point C*: reference electrode (chosen randomly at the surgeon’s discretion among the pointer electrodes). *Point D*: projection point of reference

electrode. *Point E*: projection point of B onto the same vertical axis with point X. *Point X*: access point. *k*: calculated length—1. *l*: measured length—1. *m*: calculated hypotenuse length—1. α : calculated angle—1. *o*: calculated length—(2) *r*: measured length—2. *n*: calculated hypotenuse length—2. β : calculated angle—2 (direction angle). γ : calculated angle—3 (access angle)

- iv. The point B can be marked on the surface by calculating the distance (*m*) and the angle (α).

Calculated hypotenuse length—1:

$$m = \sqrt{k^2 + l^2}$$

Calculated angle—1:

$$\alpha = \arctan\left(\frac{l}{k}\right)$$

- v. Another point (*E*) has to be determined, where point B is projected onto the same vertical axis with point X (the access point) (in other words, the point used for calculation where X is projected to be on the same horizontal axis with B).

- vi. The distance between B and E (*o*) is calculated by multiplying the difference between DICOM number of the point B and DICOM number of the projection of the point E with CT slice interval (*s*).

Calculated length—2:

$$o = (\#DICOM_B - \#DICOM_E) \times s$$

- vii. The distance between X and E (*r*) can be measured with the “LINES” command of the DICOMVCL application.

Measured length—2:

$$r = \text{LINES}(X - E)$$

- viii. The point X can be marked on the surface by calculating the distance (*n*) and the direction angle (β).

Calculated hypotenuse length—2:

$$n = \sqrt{o^2 + r^2}$$

Calculated angle—2 (direction angle):

$$\beta = \arctan\left(\frac{r}{o}\right)$$

- ix. The vertical distance between the stone (point A) and the surface projection point of the stone (point B) can be measured on the CT image. And then the access angle (γ) can be calculated.

Calculated angle—3 (access angle):

$$\gamma = \arctan \left(\frac{n}{p} \right)$$

In the first experimental model, a real kidney stone was placed in a gel cushion and a CT scan of the cushion was taken. By using the DICOM objects generated from the CT scan, the projection point of the stone was determined on the surface of the cushion, and the distance between this point and reference electrode was measured (“PCNL Calculation program”) (Fig. 2a–c). Afterwards, the access point, direction angle and access angle were calculated by using the novel mathematical calculation software (“PCNL Vectoral 3D application”) and vectoral 3D modeling was performed to point the access point on the surface (Fig. 2d).

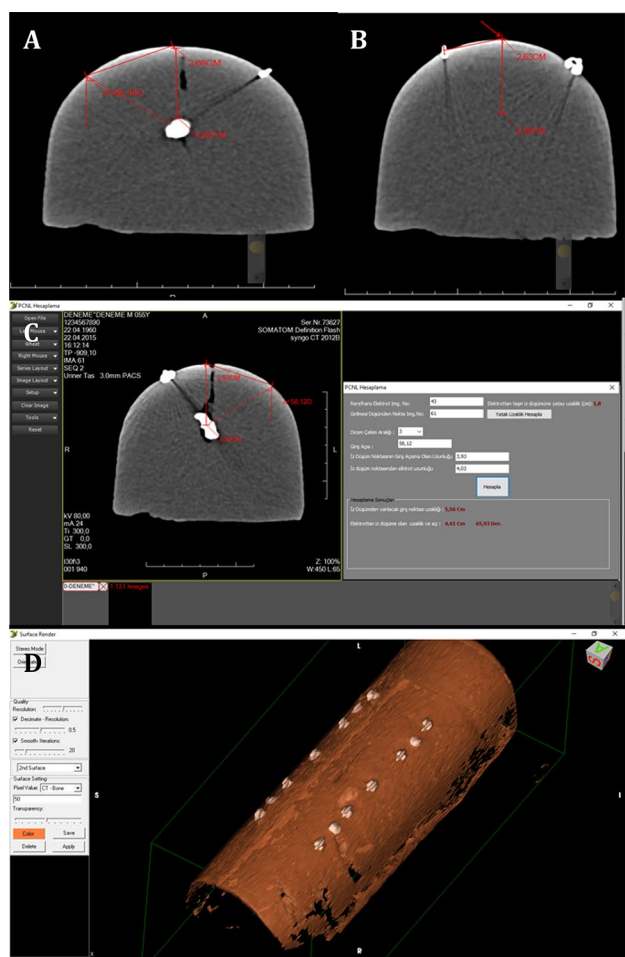


Fig. 2 First experimental model. **a** Coronal section of a stone embedded in gel cushion. **b** The projection point of the stone was determined on the surface of the cushion. The distance between this point and reference electrode was measured. The red arrow shows the intersection point of the reference electrode and projection of the stone. **c** Then the access point and angle were calculated by using the novel mathematical calculation software. **d** Vectoral 3-dimensional (3D) modeling was performed to point the access point on the surface

DICOM files were converted to STL format by the 3D Slicer program (The Slicer Community, Boston, MS, USA), and then “threshold adjustment” was performed, which determined the appearance of the 3D model (Fig. 3a, b). The STL format files were converted to FBX/OBJ files by Cinema 4D (MAXON Computer GmbH, Friedrichsdorf, Germany). Conversion of the files into FBX/OBJ format provided the data to be used in AR technology.

A “special object” had to be created and introduced to the system, which would be used by the AR library to identify the gel cushion. The FBX/OBJ format files were then transferred to Unity3D program (Unity Technologies, San Francisco, CA, USA) to be used in AR. With ObjectTarget and ARCamera (the components of Unity3D), a plane was created automatically to place the “special object” virtually onto the real object on the screen of a tablet (Fig. 3c). This process was performed by using the distance between two electrodes as a reference. The 3D modeling was placed virtually onto the real object, and the calculated access point and an access needle according to the calculated direction angle and access angle were displayed virtually on the object on the screen of the tablet (Fig. 3d).

Results

The developed system was tested on two different models. Firstly, a real kidney stone was placed in a gel cushion. After receiving a CT scan of the cushion, the calculations and 3D modeling were performed (Figs. 2, 3).

The second experimental model was made by inserting a urinary stone in a bovine kidney that was placed in a chicken (Fig. 4a–d), which has been proposed as a biological teaching model for ultrasound- or fluoroscopy- guided access in PCNL by Hacker et al. [20].

The system was tested on both experimental models for twice, and the correct access point, direction angle and access angle were achieved at every time. The accuracy of the insertion of the TLA access needle was checked by both feeling the crepitation on the stone surface and observing the tip of the needle touching the stone in a control CT scan (Fig. 4e–g).

The flowchart of the newly developed technique is shown in Fig. 5. With this novel system, the pre-operative planning and preparation can be performed easily, and the approximate required time for each step of the calculation and modeling is given below:

- Acquisition of CT images and preparation of DICOM files: 20 min
- Vectoral identification of access point in DICOM application and calculation of access point, direction angle, and access angle: 10 min

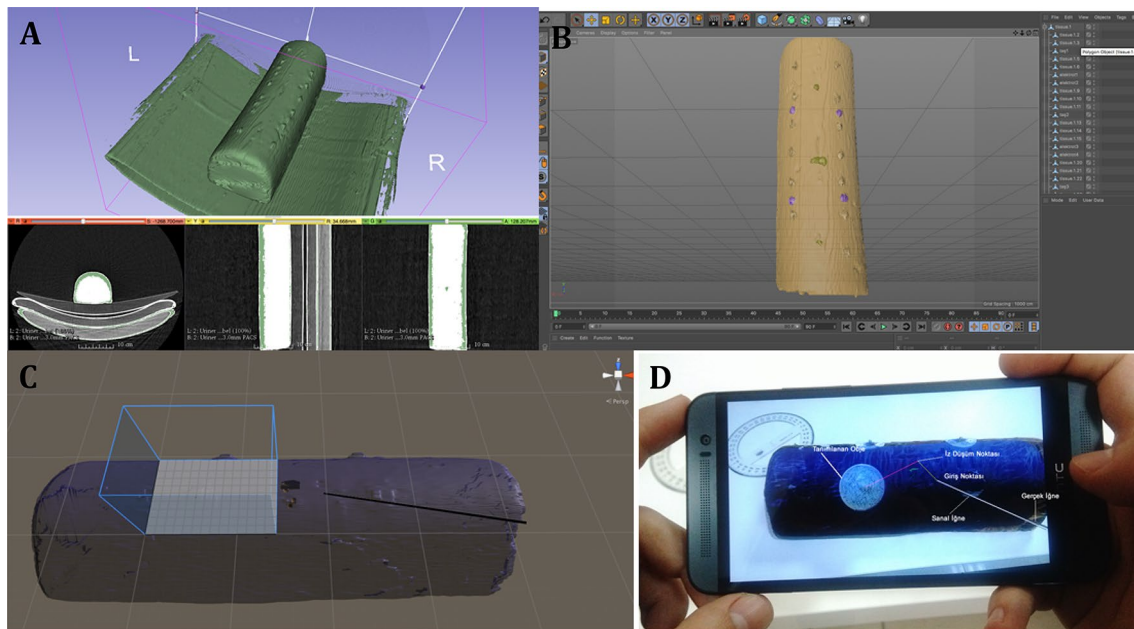


Fig. 3 First experimental model (continued). **a** Threshold adjustment and 3-dimensional (3D) modeling of the gel cushion. **b** Completed threshold adjustment and 3D modeling. **c** A “special object” was created and introduced to the system, which was used by the augmented reality library to identify the gel cushion, and a plane was created

- Conversion of the CT images (DICOM files) to STL files (for 3D images): 10 min
- Conversion of the 3D images (STL files) to FBX/OBJ files (to be used in AR): 10 min
- Upload of AR file to the tablet: 5 min

Discussion

Performing an appropriate and successful access is the critical step in PCNL that has dramatic impacts on the overall outcome of this operation. Three-dimensional imagination of the renal and perirenal anatomy is challenging as fluoroscopy or ultrasound gives 2-dimensional anatomical data. Ultrasound-guided access has a disadvantage of incomplete and single-plane visualization of the anatomical structures, limited ability to delineate fine detail of kidney and stone (particularly in obese patients or those with non-dilated collecting systems), operator dependence, and restricted spatial and contrast resolution. However, it has the ability to identify nearby organs such as bowel, spleen, or liver, and neither the patient nor the surgeon is exposed to radiation. On the other hand, fluoroscopy-guided access, most commonly used technique, provides a better visualization of the stone and collecting system with a higher resolution at the expense of higher radiation exposure of the surgeon, patient and operating room staff.

automatically to place the “special object” onto the real object. **d** The 3D modeling was placed onto the real object, and calculated access point and a virtual access needle according to the calculated direction angle and access angle were marked and placed on the object on the screen of a smart phone

Several mechanical devices and navigation concepts have been proposed to ensure an easier and more successful access with an effort to decrease radiation exposure [8–19]. Historically, Mozer et al. were the first to describe a computer-assisted technique to facilitate access by projecting the ultrasound puncture tract virtually onto pre-operative fluoroscopic images; however, only the results achieved first on a phantom and then on one patient were reported [11]. Oliveira-Santos et al. described the design and workflow of a stereotactic needle guidance system for PCNL with promising preliminary results of tests on prototype phantoms [13]. Huber et al. published their “rendezvous” technique using electromagnetic tracking in porcine ex-vivo model, and Rodrigues et al. reported their in vivo experience with a new real-time electromagnetic tracking system [15, 16].

However, image-guided navigation techniques have drawn more attention. Müller et al. introduced a model—“iPad-assisted technique”—for the concept of computer-assisted percutaneous access, with intent to integrate this into routine clinical use [18]. In their phantom study, collecting systems of the porcine kidneys embedded in ballistic gelatin were punctured under iPad, ultrasound and fluoroscopy assistance, and mean radiation exposure and median puncture time of one inexperienced and two experienced urologists were compared. Better results with iPad assistance for puncture time and radiation exposure were observed for the urological trainee than the experienced

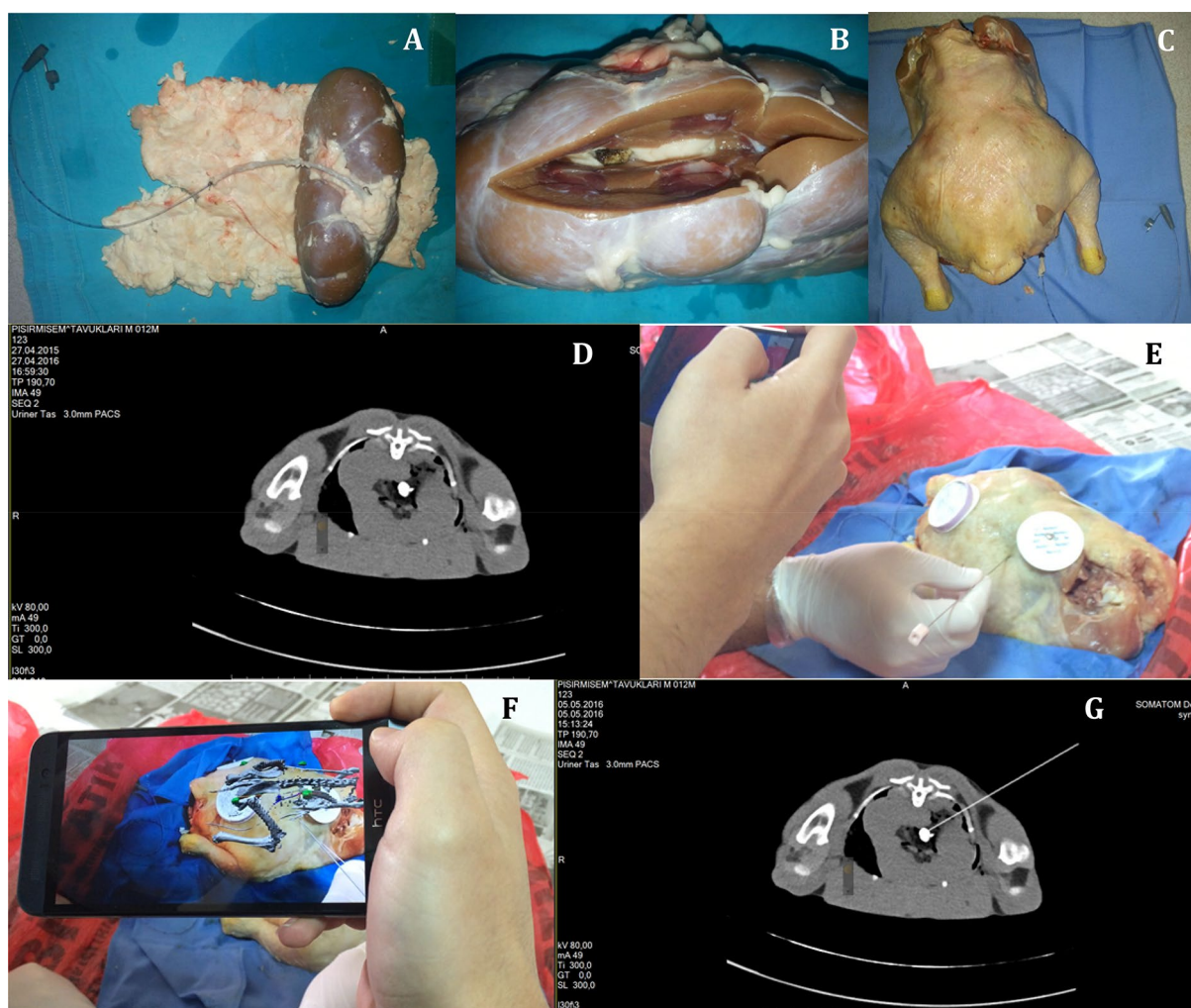


Fig. 4 Second experimental model. **a–c** Preparation of the model by inserting a urinary stone in a bovine kidney that is placed in a chicken. **d** CT image of the stone located in the bovine kidney. **e–f**

Insertion of the TLA needle into the bovine kidney with the aid of augmented reality image on a smart phone. **g** CT image proving that the TLA needle touches the stone

urologists, which was interpreted by the familiarity of the experts with the standard equipment. They concluded that this novel technique was comparable with the previously reported techniques [14, 15, 17] in terms of puncture time. It was also reported that iPad assistance enabled to gain an optimal access in a one-step puncture in the initial clinical test performed on two patients [21].

Recently, Li et al. published a pre-operative planning technique for PCNL using construction of 3D model of kidney, stone, vasculature and adjacent organs [19]. Pre-operative CT images for unenhanced, arterial, venous, and excretory phases were obtained from 15 patients, and image segmentation was performed by a 3D reconstruction software. They reported that this comprehensive pre-operative planning ensured to achieve a one-stage stone-free rate of 93.3% and made the surgeon feel more confident and comfortable during the puncture.

Although our novel technique seems to be a combination of the techniques described by Müller et al. [18] and Li et al. [19], it has some major differences. We have developed new software to calculate the access point and angle, which has not been yet done by anyone else. In both experimental models for each time, the stone was successfully touched by the needle by using this novel calculation.

In their technique, Müller et al. used image capture with a proactive camera, recognition of the object with image processing, compression of this processed data and then transmission to main computer by using local area network (LAN) [18]. This enabled production of an instant AR image that can be continuously adjusted according to the position of the object and the camera. Apart from this dynamic setting, our technique did not require a main computer with too much hardware, a well structured LAN

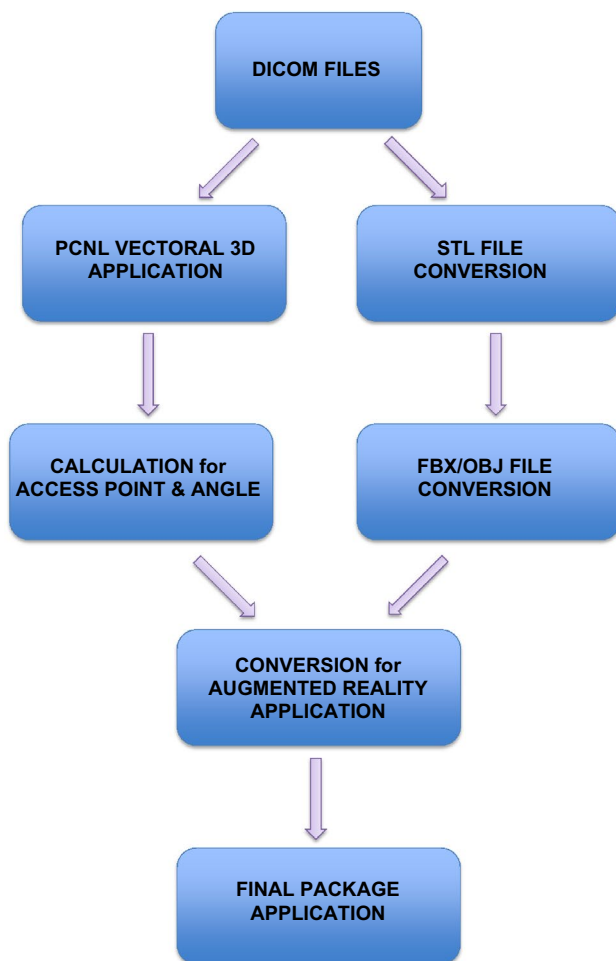


Fig. 5 The flowchart of the novel technique

and compression–transmission–decompression of images. Therefore, we did not observe a target visualization error.

Although we herein report only our preliminary experimental results, we used real patient data to develop the novel software. At first, we used the same CT protocol that Li et al. used [19]. After analyzing the CT scans and using them to create 3D modeling, we concluded that venous phase CT scan did not give us additional data. Moreover, with the dual-source dual-energy property of the CT device, we were able to get virtual non-enhanced image of the stone. Therefore, unlike what Li et al. [19] did, we omitted unenhanced and venous phase scans and performed only two scans (arterial and excretory phase) of the patients in which the boundaries of the scanned region (limited to the kidneys and reference electrodes) was determined according to the scout image taken at the beginning. Although it is not in the scope of this paper, these modifications would obviously decrease the total radiation exposure of the patient.

The proposed novel modality has some more advantages. We did not use expensive commercially available software

(such as 3D Doctors, Mimics), which decreased the total cost of the system. Moreover, instead of an expensive CT device (i.e., Uro Dyna-CT) that not every center can afford, this technique can be performed with a CT device that can be available in every hospital, even with a non-dual-energy setting. It also differs from the techniques using electromagnetic tracking systems, as it does not require any sophisticated equipment.

It seems that young urologists have a hesitation to perform the access on their own after their residency. A recent study showed that three-quarters of the practicing urologists in the North Central Section of the American Urological Association (AUA) who responded to a survey reported feeling comfortable while performing PCNL, but only 11% of that group routinely obtained percutaneous access without the assistance of a radiologist [22]. Furthermore, Lee et al. demonstrated that urologists who have trained on percutaneous access during their residency performed more percutaneous surgery than whom have not trained, and only a small portion from both groups continued to perform percutaneous access on their own (27% trained vs. 11% untrained) [23]. We think that when this system is further developed, it will facilitate performing the crucial step of PCNL, which can be of benefit for trainees and/or novice surgeons.

The goal of this system is to ensure a correct access point and angle in PCNL with a perfect overlay of the AR image of the structures onto the patient's skin on the screen of a smartphone/tablet and without use of fluoroscopy when it is incorporated to routine clinical use. Although this has been achieved in the above-mentioned experimental models, a spatial error may occur because of the complex surface anatomy of the lumbar region and body habitus in humans. Moreover, the slight movement of the kidney/stone during respiration and/or the deformation on the skin while the needle is introduced may cause a difficulty during a real PCNL operation. As this is a bench-top study, it does not take into account all the variables that would be encountered during an in vivo setting. Therefore, the initial effective application and promising results of this technique must be viewed in light of these limitations of the study.

Although we have not yet tested this technique on humans, our aim for developing this technique was to ensure a correct, reliable, and safe puncture for the access during PCNL not only in patients with normal anatomy, but also the ones with abnormal anatomy, such as ectopic, malrotated, or horseshoe kidneys, and patients with radiolucent stones. As radiolucent stones are also visible on CT, and vast majority of PCNL patients (with either radiopaque or radiolucent stone, or with abnormal anatomy) undergo a CT pre-operatively, we expect this technique to be feasible and usable in these challenging cases as long as an appropriate CT is obtained, and required calculations and modeling are performed by using this CT. Moreover, we think this

technique may be used for gaining access into a superior calyx using an infracostal puncture.

The calculated results do not depend on the position of the smartphone or tablet. These results depend on how the CT is taken; therefore, it is important to take the CT under similar conditions as possible as PCNL is performed. On the other hand, the results depend on the technical properties of smartphone/tablet, such as its processor and camera resolution, which are important for detection of image under bright light, and the perfect overlay of the AR image of the structures onto the patient's skin on the screen of a smartphone/tablet.

As the skeletal structures (ribs, vertebrae, and pelvic bones) can be observed clearly in the 3D modeling and AR image, in case the calculated access point just sits on a rib, which makes it impossible to gain access through it, a new access point can be calculated by changing the touching point (targeted point on stone surface or puncture point of the collecting system) a few millimeters, without compromising the success of the operation as this operation is generally performed for relatively large stones (> 2 cm). Moreover, when touching a stone is not the desired plan, such as puncturing a calyx that does not contain a stone (i.e., in case of an anteriorly located stone) or puncturing a calyx that contains one of the stones (smaller stone) in case of multiple stones, this technique may also be used by defining the 'non-stone-bearing optimal' calyx as the targeted access point.

In conclusion, this novel device, which uses software-based mathematical calculation, 3D modeling, and AR technology, seems to ensure a correct access point and angle for PCNL. However, the preliminary results obtained from two different ex-vivo models are not enough to foresee its clinical utility, and it is obvious that further work is required to make this technique advanced, to demonstrate its clinical safety and efficacy, and to test its suitability for different scenarios.

Acknowledgements We would like to thank Yunus Emre KIYMAZ (PhD student), Ibrahim Hakan UGRAS, Selman KIRBAG and Emre BUYUKASLAN for their invaluable contributions to the study.

Funding This project was funded by The Scientific and Technological Research Council of Turkey (TÜBİTAK) with the Grant No. 114S348.

Compliance with ethical standards

Conflict of interest All authors declare that they have no conflict of interest or financial ties to disclose.

Ethical approval All procedures performed in studies involving human participants were in accordance with the ethical standards of the institutional and/or national research committee and with the 1964 Helsinki declaration and its later amendments or comparable ethical standards. The study design was approved by the Selcuk University School of Medicine Ethics Committee (approval number: 2013/7, approval date: 13.03.2013).

Informed consent Informed consent was obtained from all individual participants included in the study.

References

1. Türk C, Knoll T, Petrik A (2015) European Association of Urology (EAU) Guidelines on urolithiasis. European Association of Urology 2015. http://uroweb.org/wp-content/uploads/22-Urolithiasis_LR_full.pdf
2. Rupel E, Brown R (1941) Nephroscopy with removal of stone following nephrostomy for obstructive calculous anuria. *J Urol* 46:177
3. Goodwin WE, Casey WC, Woolf W (1955) Percutaneous trocar (needle) nephrostomy in hydronephrosis. *J Am Med Assoc* 157:891–894
4. Fernström I, Johansson B (1976) Percutaneous nephrolithotomy: a new extraction technique. *Scand J Urol Nephrol* 10:257–259
5. Wickham JE, Kellett MJ (1981) Percutaneous nephrolithotomy. *Br J Urol* 53:297–299
6. Preminger GM, Tiselius HG, Assimos DG, Alken P, Buck C, Gallurci M, Knoll T, Lingeman JE, Nakada SY, Pearle MS, Sarica K, Türk C, Wolf JS Jr, EAU/AUA Nephrolithiasis Guideline Panel (2007) 2007 guideline for the management of ureteral calculi. *J Urol* 178:2418–2434
7. Andonian S, Scoffone C, Louie MK, Gross AJ, Grabe M, Daels FP, Shah HN, de la Rosette JJ, CROES PCNL Study Group (2012) Does imaging modality used for percutaneous renal access make a difference? A matched case analysis. *J Endourol* 27:24–28
8. Su LM, Stoianovici D, Jarrett TW, Patriciu A, Roberts WW, Cadeddu JA, Ramakumar S, Solomon SB, Kavoussi LR (2002) Robotic percutaneous access to the kidney: comparison with standard manual access. *J Endourol* 16:471–475
9. Challacombe B, Patriciu A, Glass J, Aron M, Jarrett T, Kim F, Pinto P, Stoianovici D, Smeeton N, Tiptaft R, Kavoussi L, Dasgupta P (2005) A randomized controlled trial of human versus robotic and telerobotic access to the kidney as the first step in percutaneous nephrolithotomy. *Comput Aided Surg* 10:165–171
10. Ko R, Razvi H (2007) C-arm laser positioning device to facilitate percutaneous renal access. *Urology* 70:360–361
11. Mozer P, Conort P, Leroy A, Baumann M, Payan Y, Troccaz J, Chartier-Kastler E, Richard F (2007) Aid to percutaneous renal access by virtual projection of the ultrasound puncture tract onto fluoroscopic images. *J Endourol* 21:460–465
12. Zarrabi AD, Conradi JP, Heyns CF, Scheffer C, Schreve K (2010) Development of a computer assisted gantry system for gaining rapid and accurate calyceal access during percutaneous nephrolithotomy. *Int Braz J Urol* 36:738–746
13. Oliveira-Santos T, Peterhans M, Roth B, Reyes M, Nolte LP, Thalmann G, Weber S (2010) Computer aided surgery for percutaneous nephrolithotomy: clinical requirement analysis and system design. *Conf Proc IEEE Eng Med Biol Soc* 2010:442–445
14. Lazarus J, Williams J (2011) The locator: novel percutaneous nephrolithotomy apparatus to aid collecting system puncture—a preliminary report. *J Endourol* 25:747–750
15. Huber J, Wegner I, Meinzer HP, Hallscheidt P, Hadaschik B, Pahernik S, Hohenfellner M (2011) Navigated renal access using electromagnetic tracking: an initial experience. *Surg Endosc* 25:1307–1312
16. Rodrigues PL, Vilaça JL, Oliveira C, Cicione A, Rassweiler J, Fonseca J, Rodrigues NF, Correia-Pinto J, Lima E (2013) Collecting system percutaneous access using real-time tracking sensors: first pig model in vivo experience. *J Urol* 190:1932–1937

17. Ritter M, Rassweiler MC, Hacker A, Michel MS (2013) Laser-guided percutaneous kidney access with the Uro Dyna-CT: first experience of three-dimensional puncture planning with an ex vivo model. *World J Urol* 31:1147–1151
18. Müller M, Rassweiler MC, Klein J, Seitel A, Gondan M, Baumhauer M, Teber D, Rassweiler JJ, Meinzer HP, Maier-Hein L (2013) Mobile augmented reality for computer-assisted percutaneous nephrolithotomy. *Int J Comput Assist Radiol Surg* 8:663–675
19. Li H, Chen Y, Liu C, Li B, Xu K, Bao S (2013) Construction of a three-dimensional model for renal stones: comprehensive planning for percutaneous nephrolithotomy and assistance in surgery. *World J Urol* 31:1587–1592
20. Hacker A, Wendt-Nordahl G, Honeck P, Michel MS, Alken P, Knoll T (2007) A biological model to teach percutaneous nephrolithotomy technique with ultrasound- or fluoroscopy-guided access. *J Endourol* 21:545–550
21. Rassweiler JJ, Müller M, Fangerau M, Klein J, Goezen AS, Pereira P, Meinzer HP, Teber D (2012) iPad-assisted percutaneous access to the kidney using marker-based navigation: initial clinical experience. *Eur Urol* 61:627–631
22. Bird VG, Fallon B, Winfield HN (2003) Practice patterns in the treatment of large renal stones. *J Endourol* 17:355–363
23. Lee CL, Anderson JK, Monga M (2004) Residency training in percutaneous renal access: does it affect urological practice? *J Urol* 171:592–595